

Supplementary Material

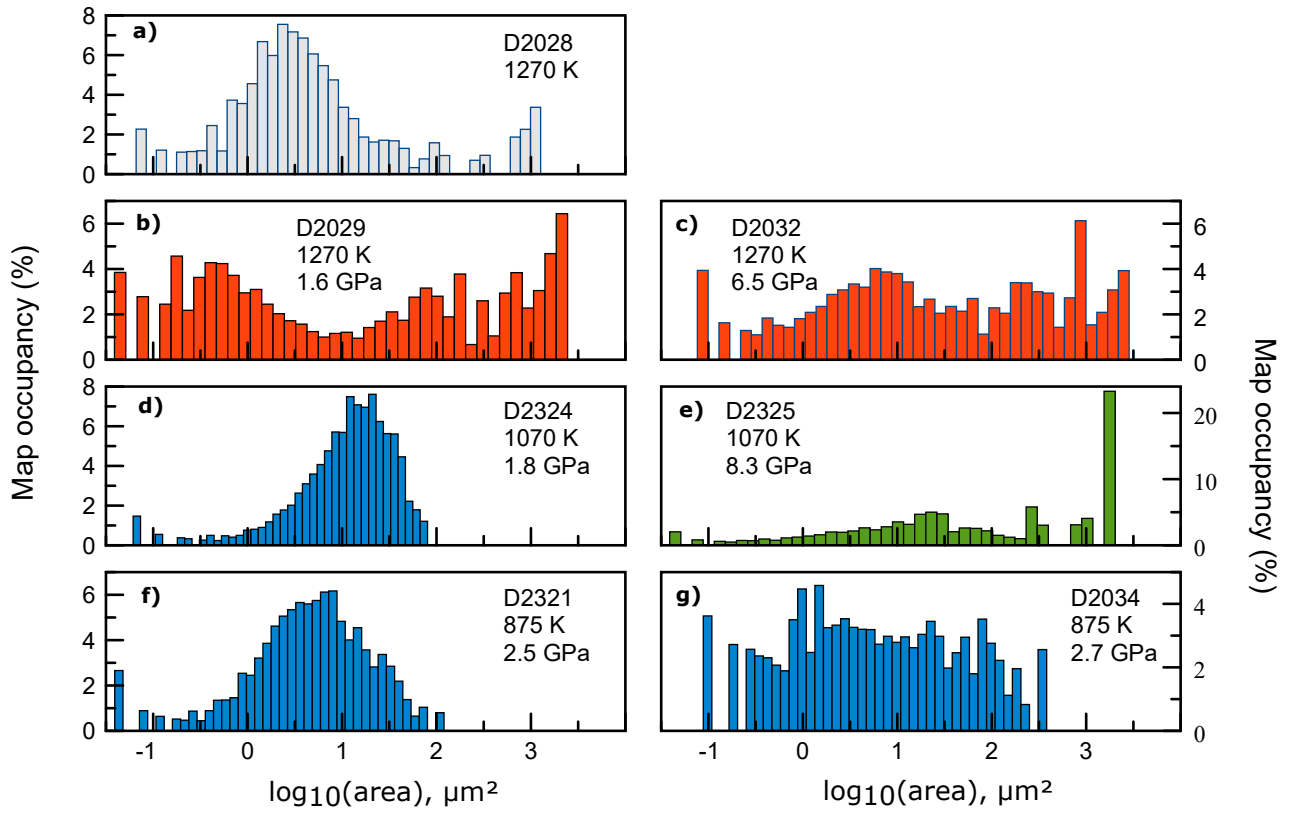


Figure S1. Grain size distribution for each MgO sample, including the reference sample (a).

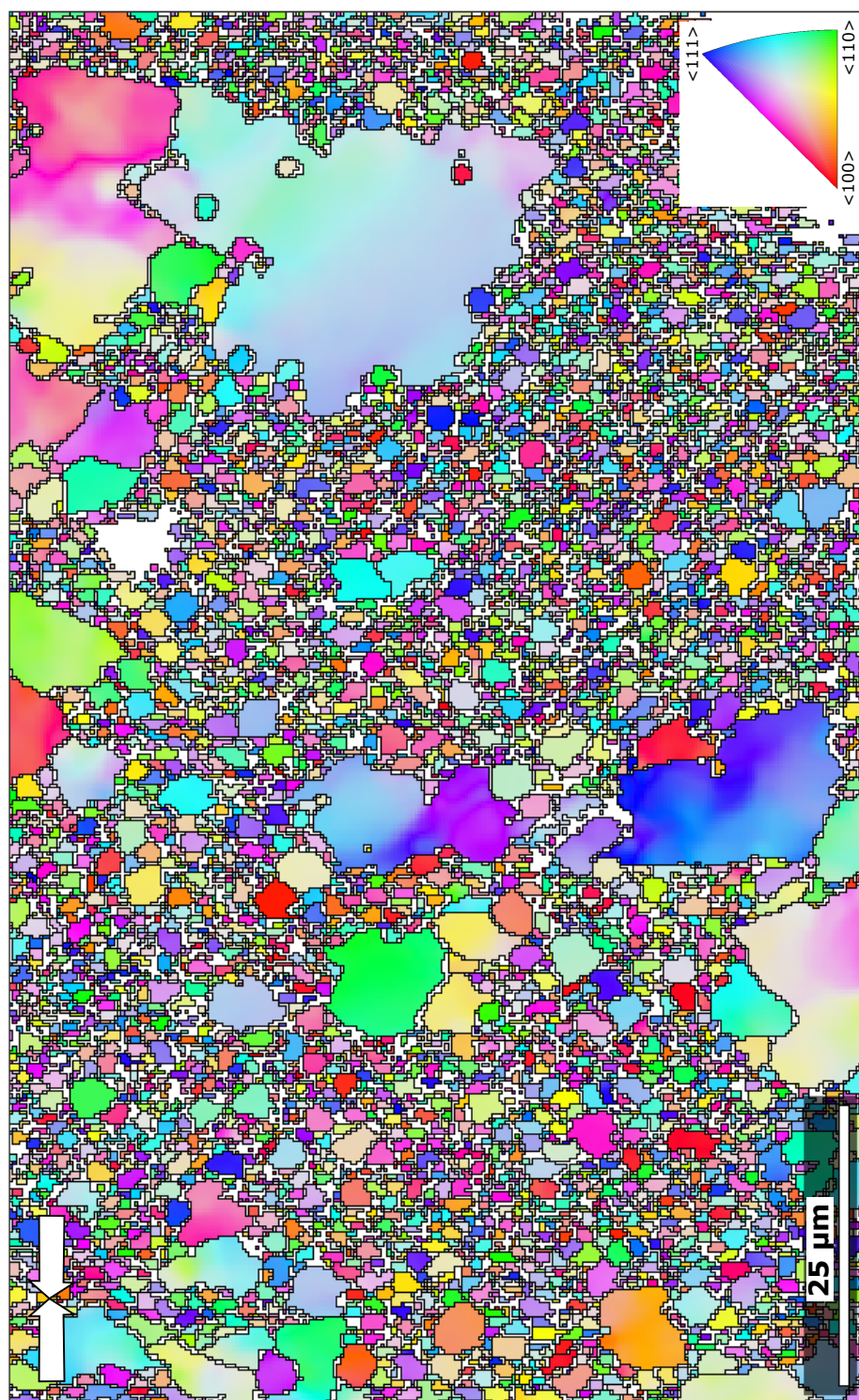


Figure S2. EBSD orientation map for sample D2029 deformed at 1270 K and 1.6 GPa, in full size. Colored after the inverse pole figure of the compression direction shown in the bottom right corner. The compression direction is indicated by the white arrows.

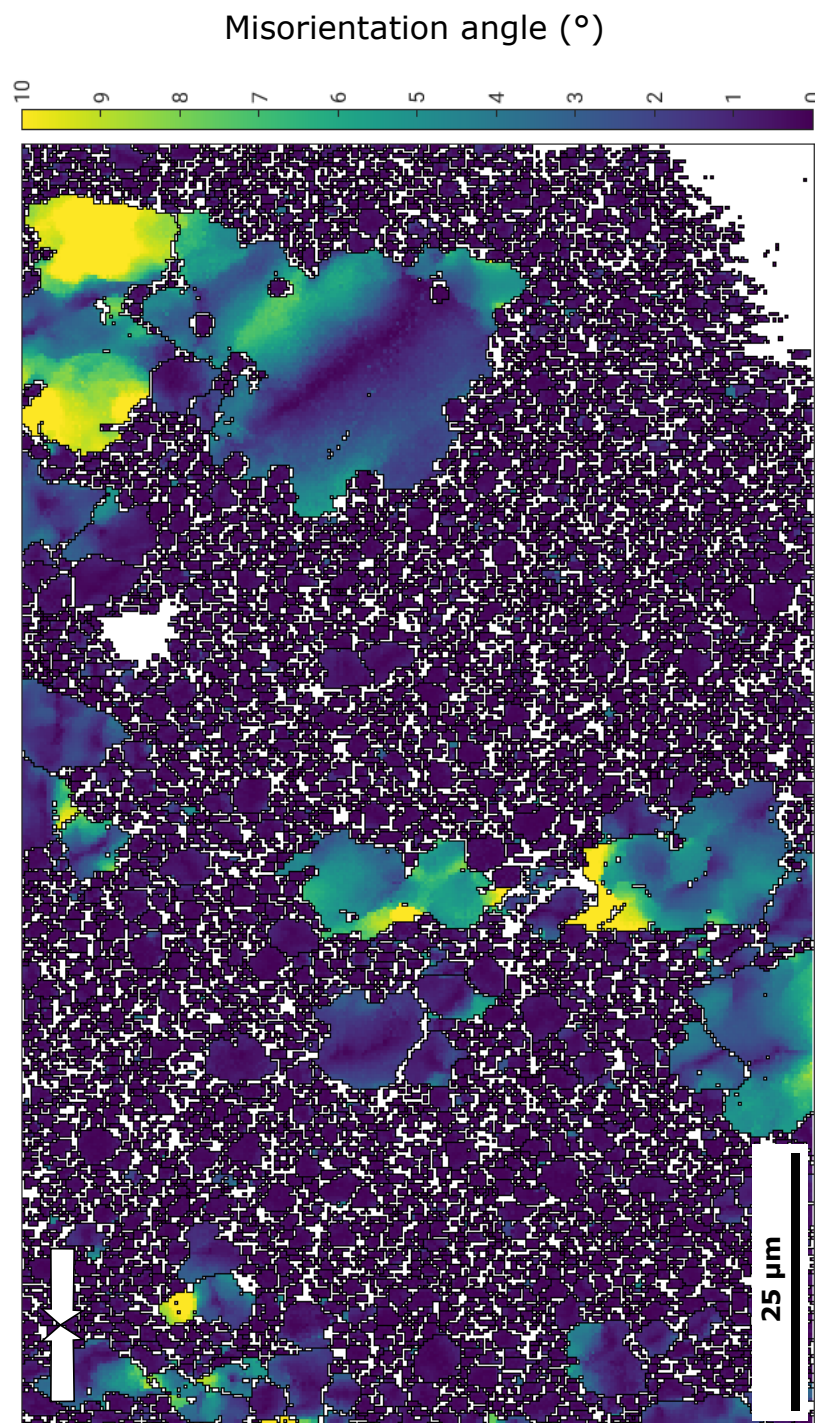


Figure S3. EBSD intracrystalline misorientation map (GROD) for sample D2029 deformed at 1270 K and 1.6 GPa, in full size. The compression direction is indicated by the white arrows.

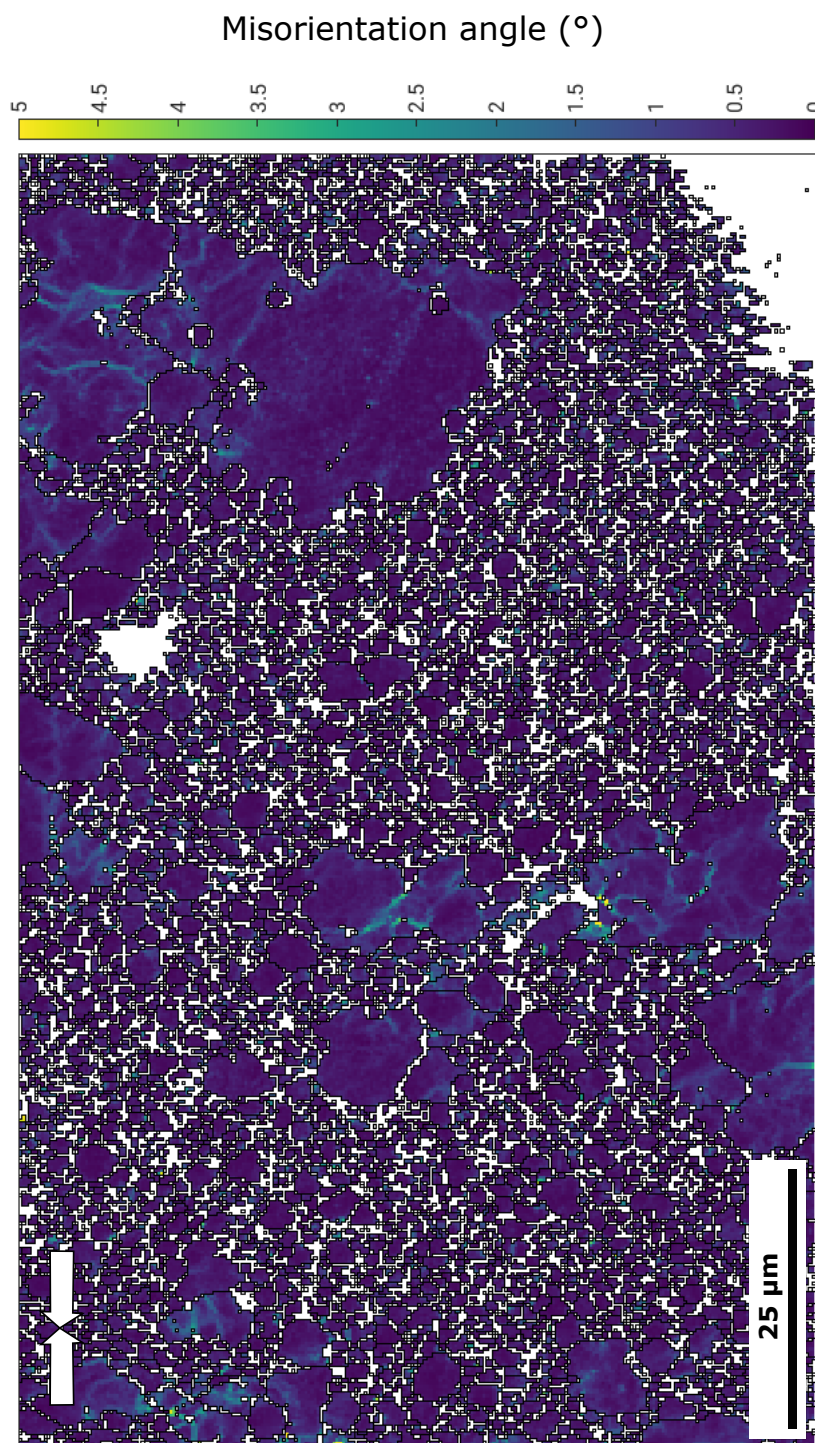


Figure S4. Local misorientation gradient (KAM) map for sample D2029 deformed at 1270 K and 1.6 GPa, in full size. The compression direction is indicated by the white arrows.

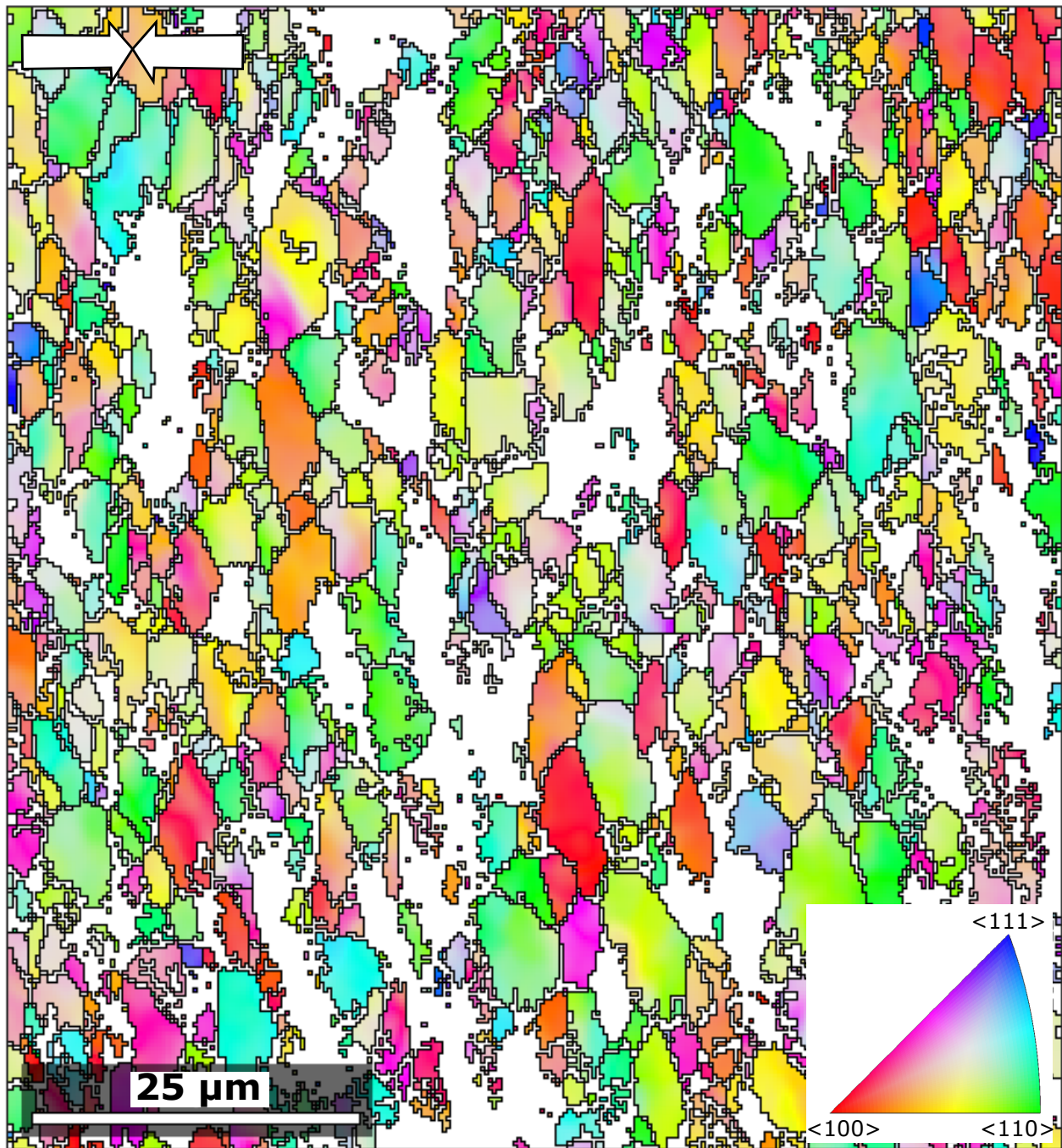


Figure S5. EBSD orientation map for sample D2324 deformed at 1070 K and 1.8 GPa, in full size. Colored after the inverse pole figure of the compression direction shown in the bottom right corner. The compression direction is indicated by the white arrows.

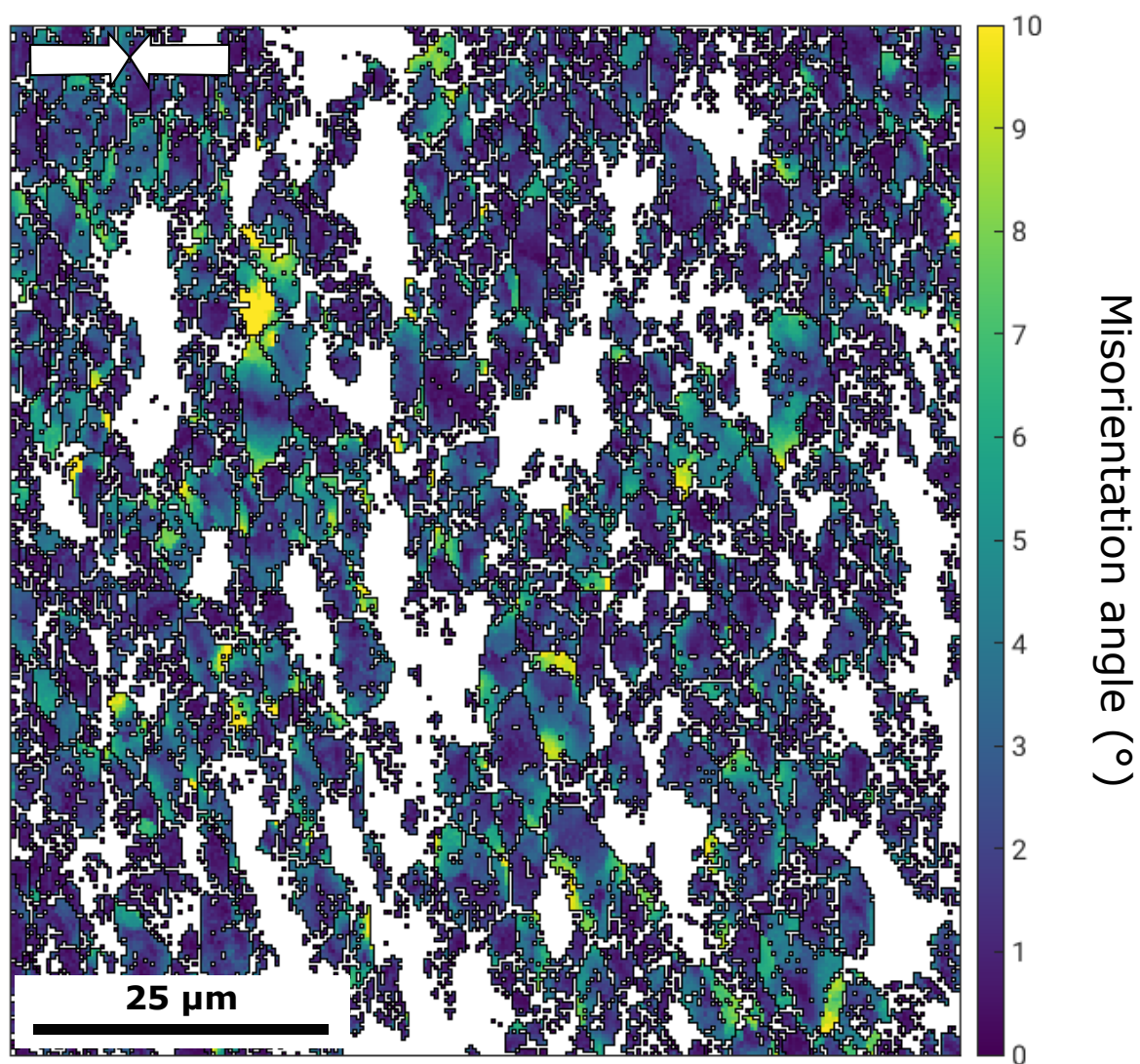


Figure S6. EBSD intracrystalline misorientation map (GROD) for sample D2324 deformed at 1070 K and 1.8 GPa, in full size. The compression direction is indicated by the white arrows.

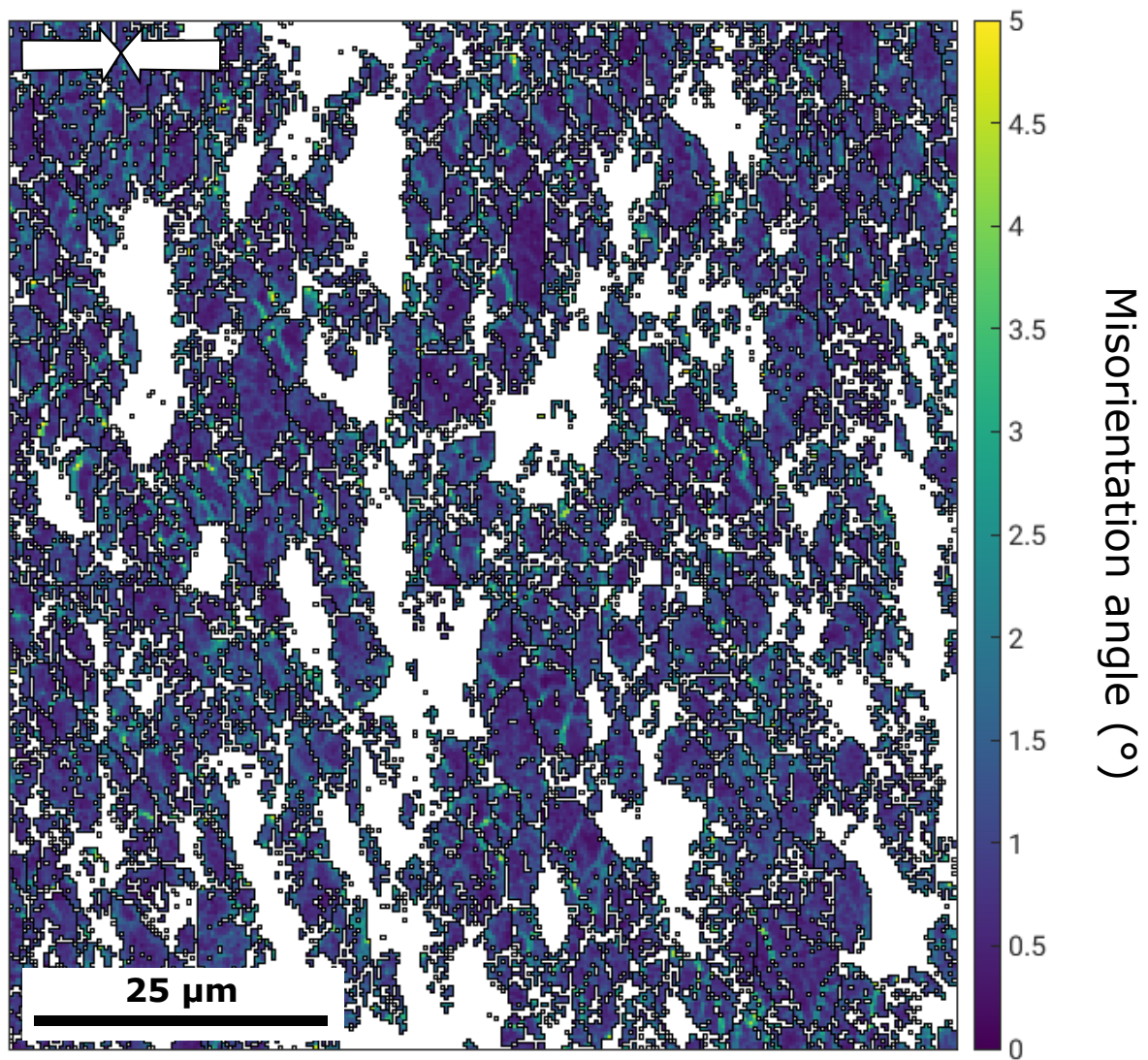


Figure S7. Local misorientation gradient (KAM) map for sample D2324 deformed at 1070 K and 1.8 GPa, in full size. The compression direction is indicated by the white arrows.

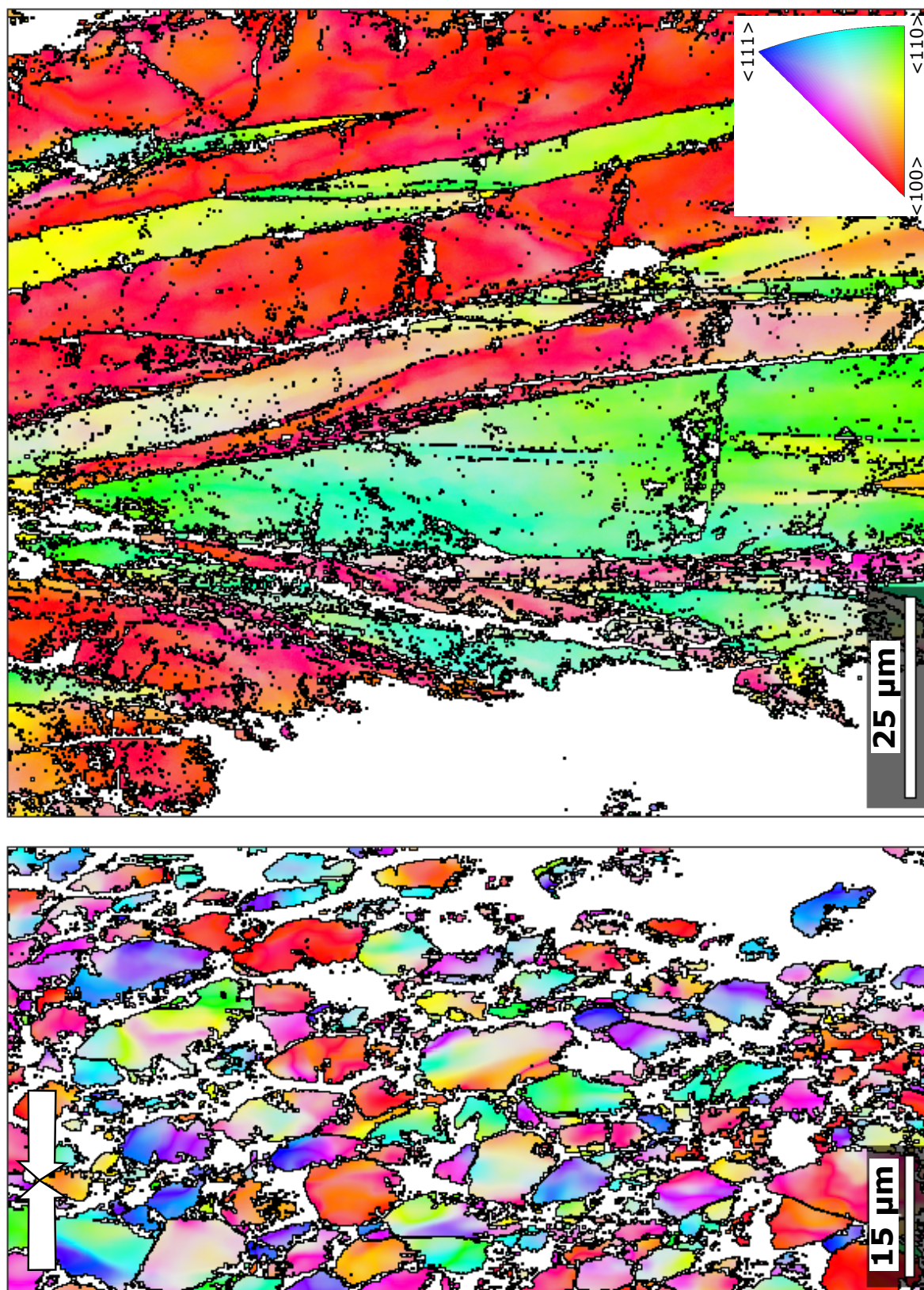


Figure S8. EBSD orientation map for sample D2325, deformed at 1070 K and 8.3 GPa, in full size. Colored after the inverse pole figure of the compression direction shown in the bottom right corner. The compression direction is indicated by the white arrows.

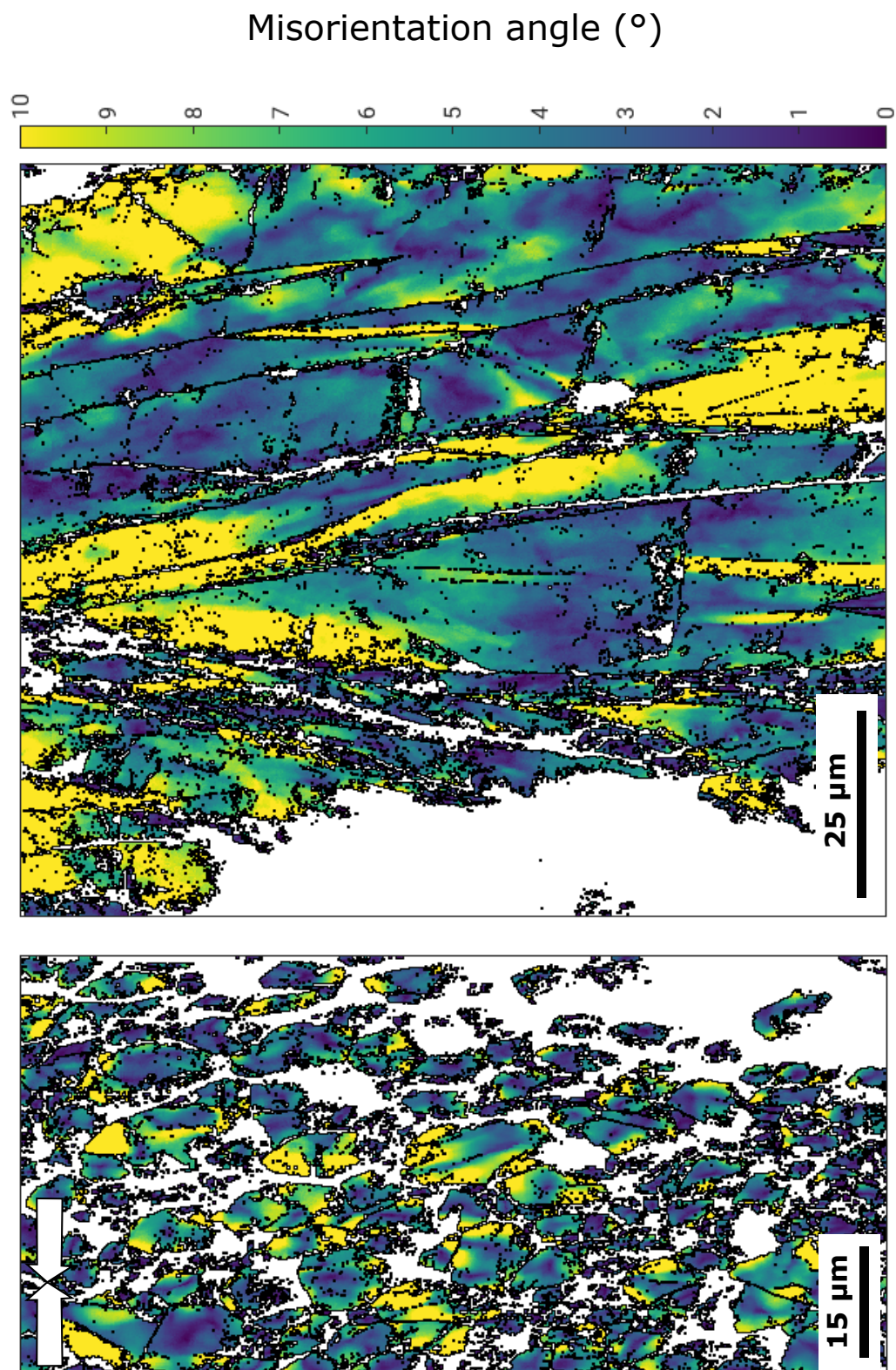


Figure S9. EBSD intracrystalline misorientation map (GROD) for sample D2325, deformed at 1070 K and 8.3 GPa, in full size. The compression direction is indicated by the white arrows.

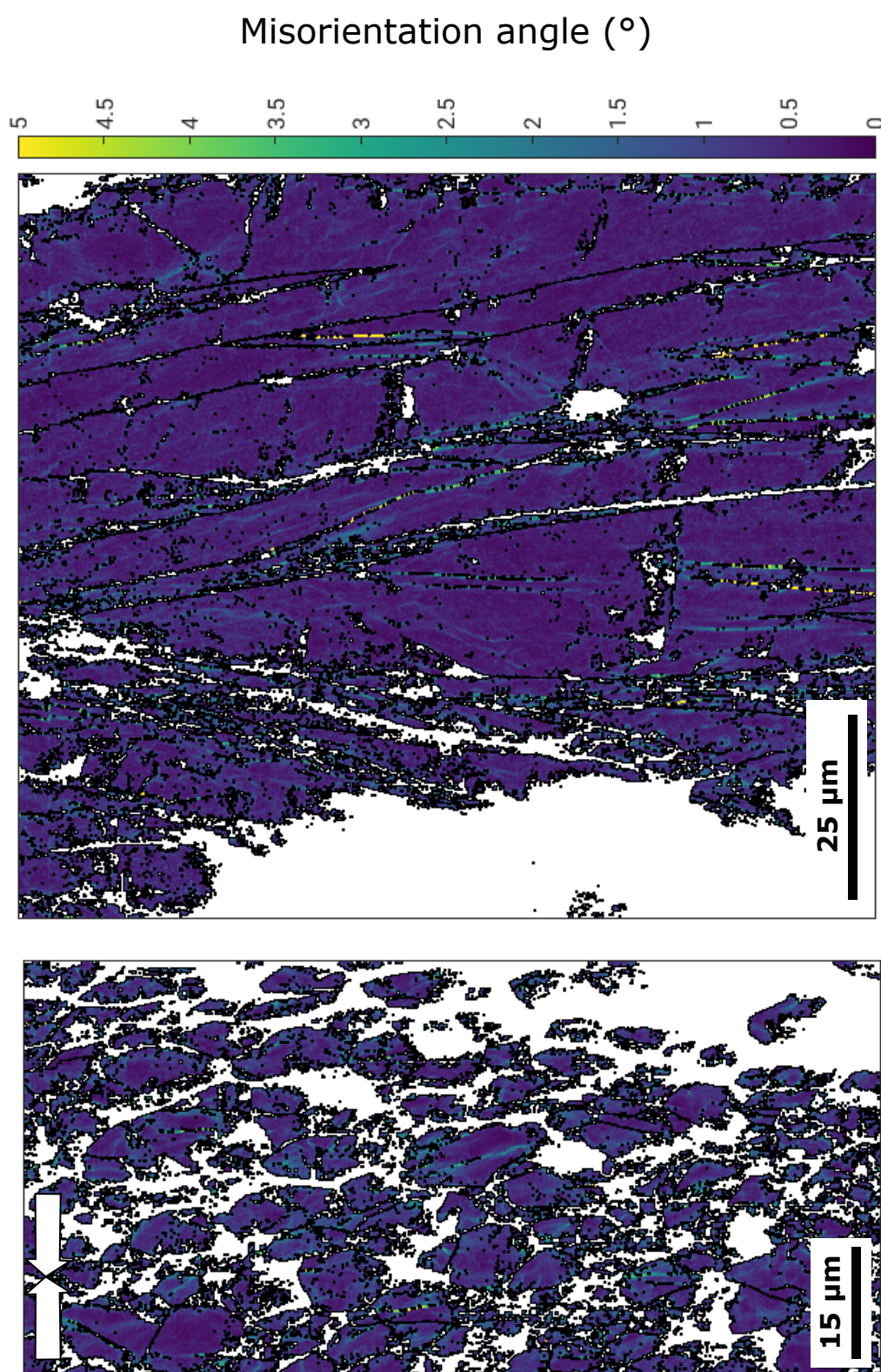


Figure S10. Local misorientation gradient (KAM) map for sample D2325, deformed at 1070 K and 8.3 GPa, in full size. The compression direction is indicated by the white arrows.

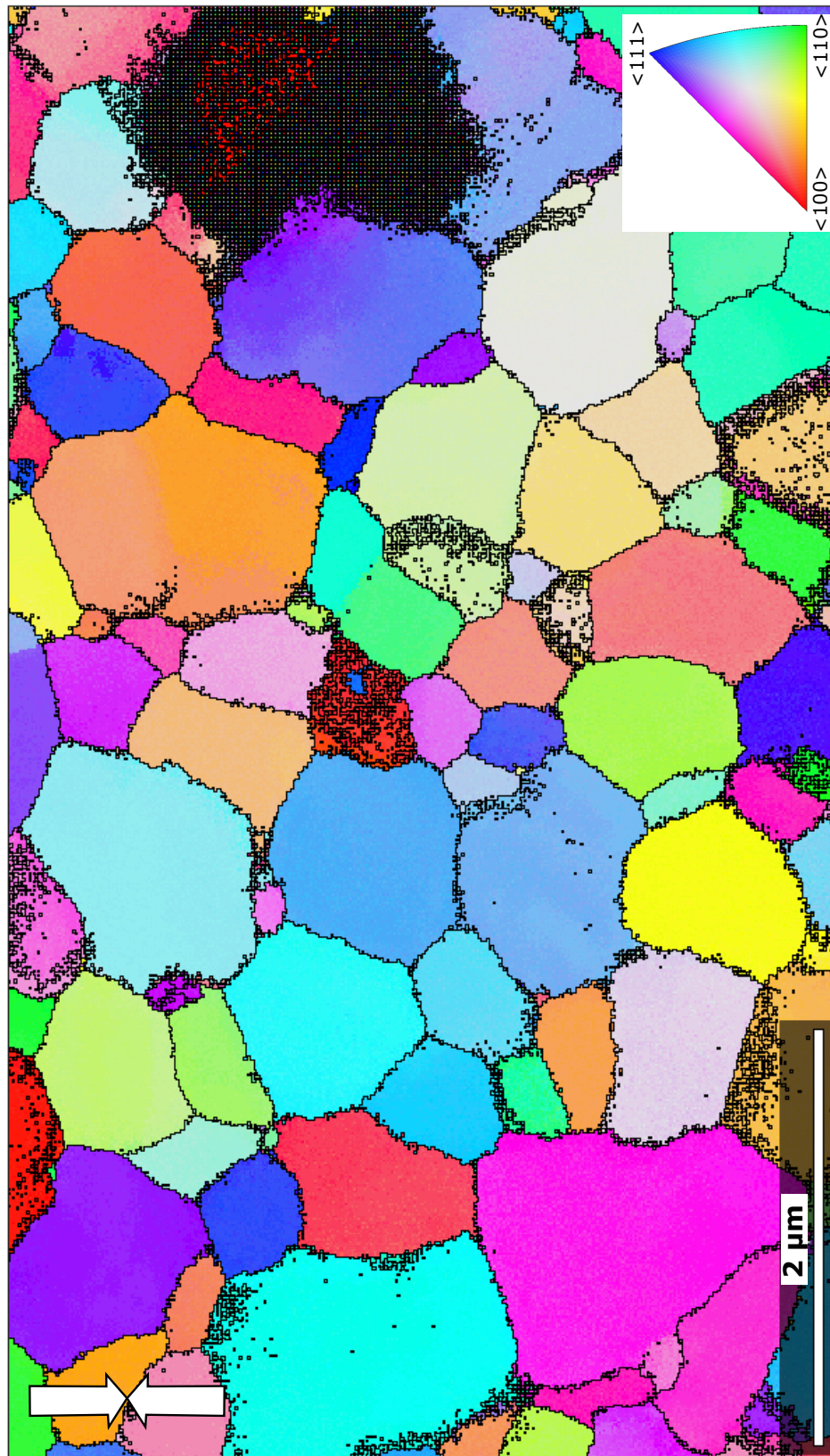


Figure S11. ASTAR orientation map for sample D2029, deformed at 1270 K and 1.6 GPa, in full size. Colored after the inverse pole figure of the compression direction shown in the bottom right corner. The compression direction is indicated by the white arrows.

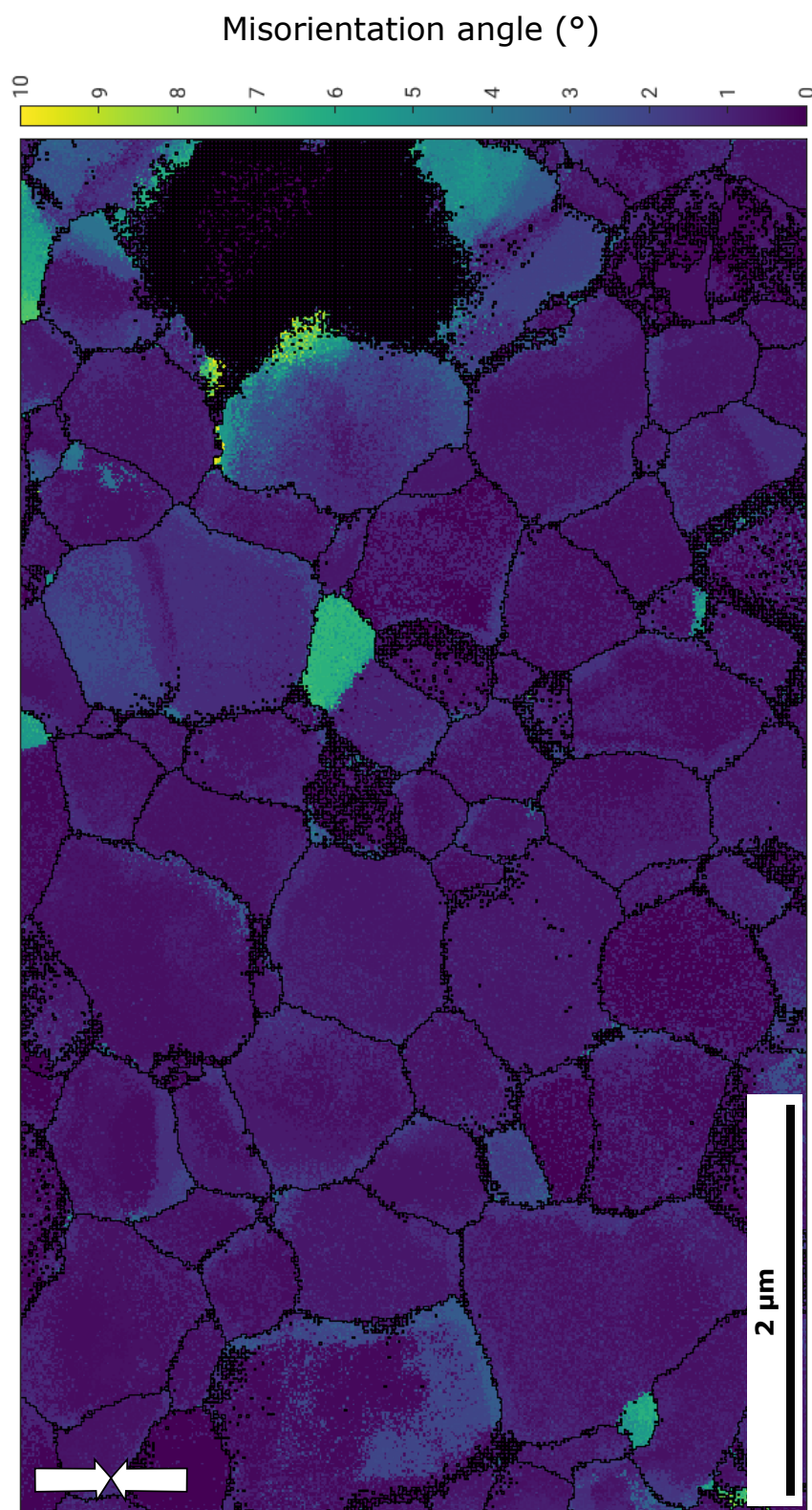


Figure S12. ASTAR intracrystalline misorientation map (GROD) for sample D2029 deformed at 1270 K and 1.6 GPa, in full size. The compression direction is indicated by the white arrows.

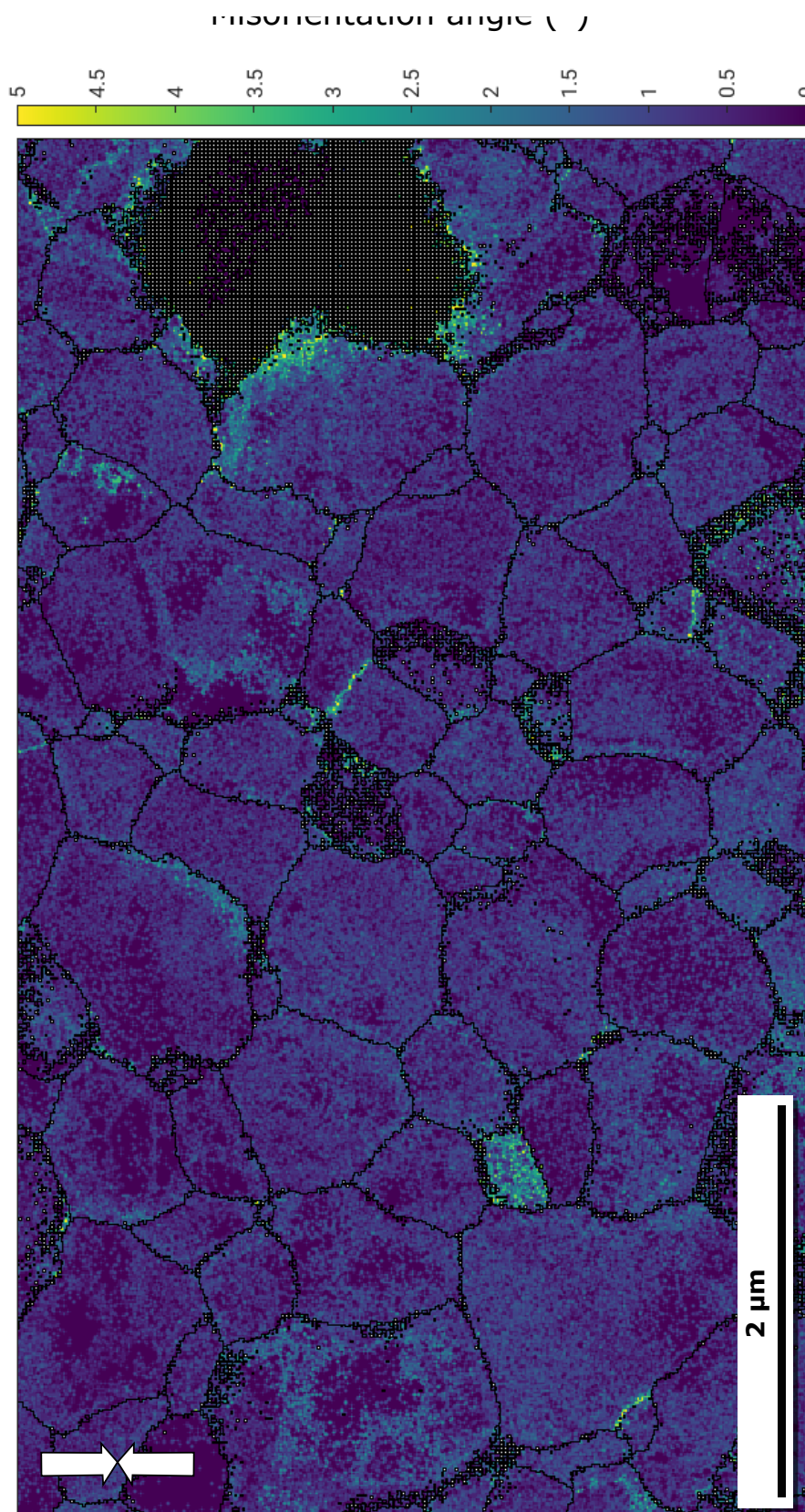


Figure S13. ASTAR local misorientation gradient (KAM) map for sample D2029, deformed at 1270 K and 1.6 GPa, in full size. The compression direction is indicated by the white arrows.

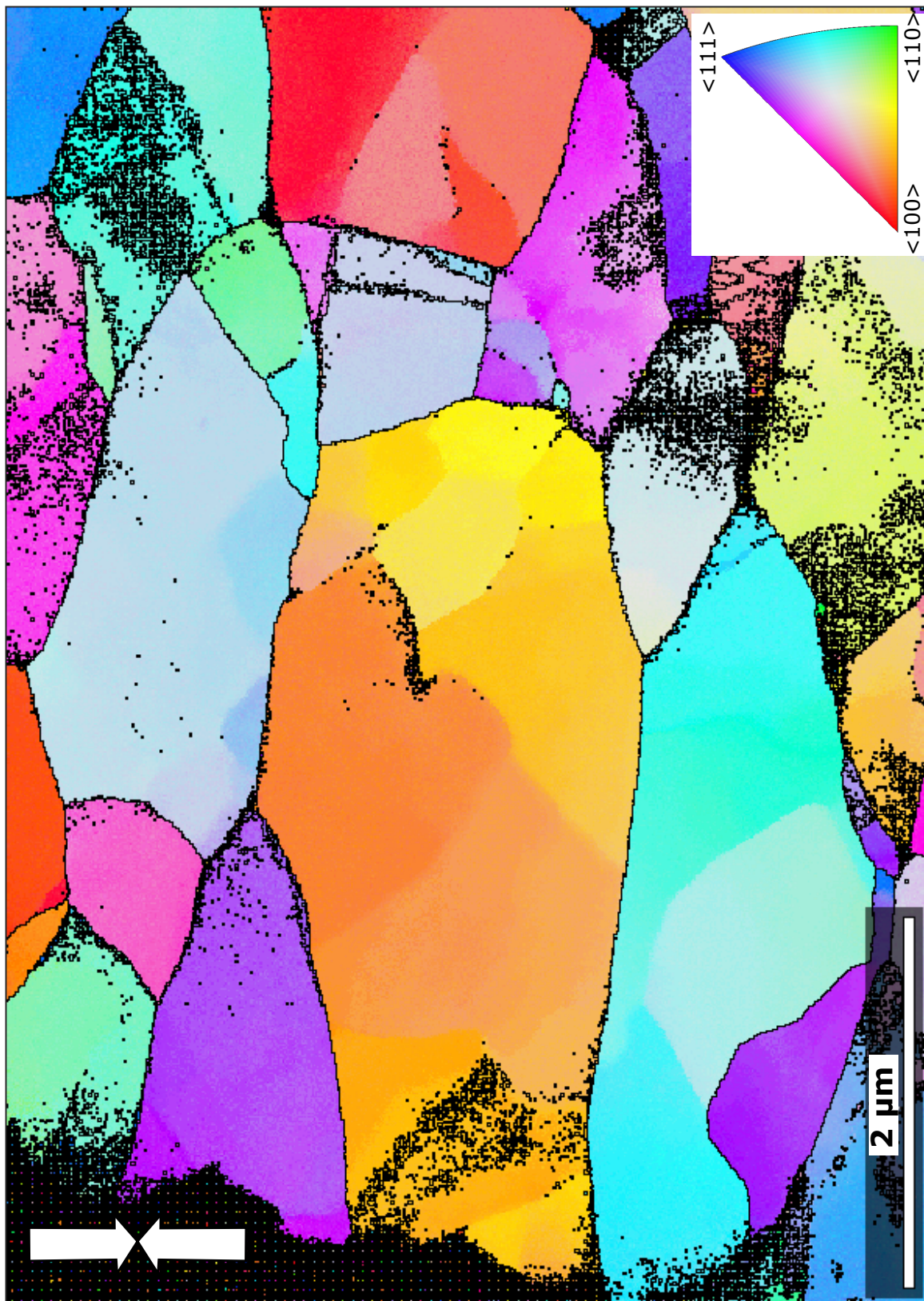


Figure S14. ASTAR orientation map for sample D2321, deformed at 1070 K and 2.5 GPa, in full size. Colored after the inverse pole figure of the compression direction shown in the bottom right corner. The compression direction is indicated by the white arrows.

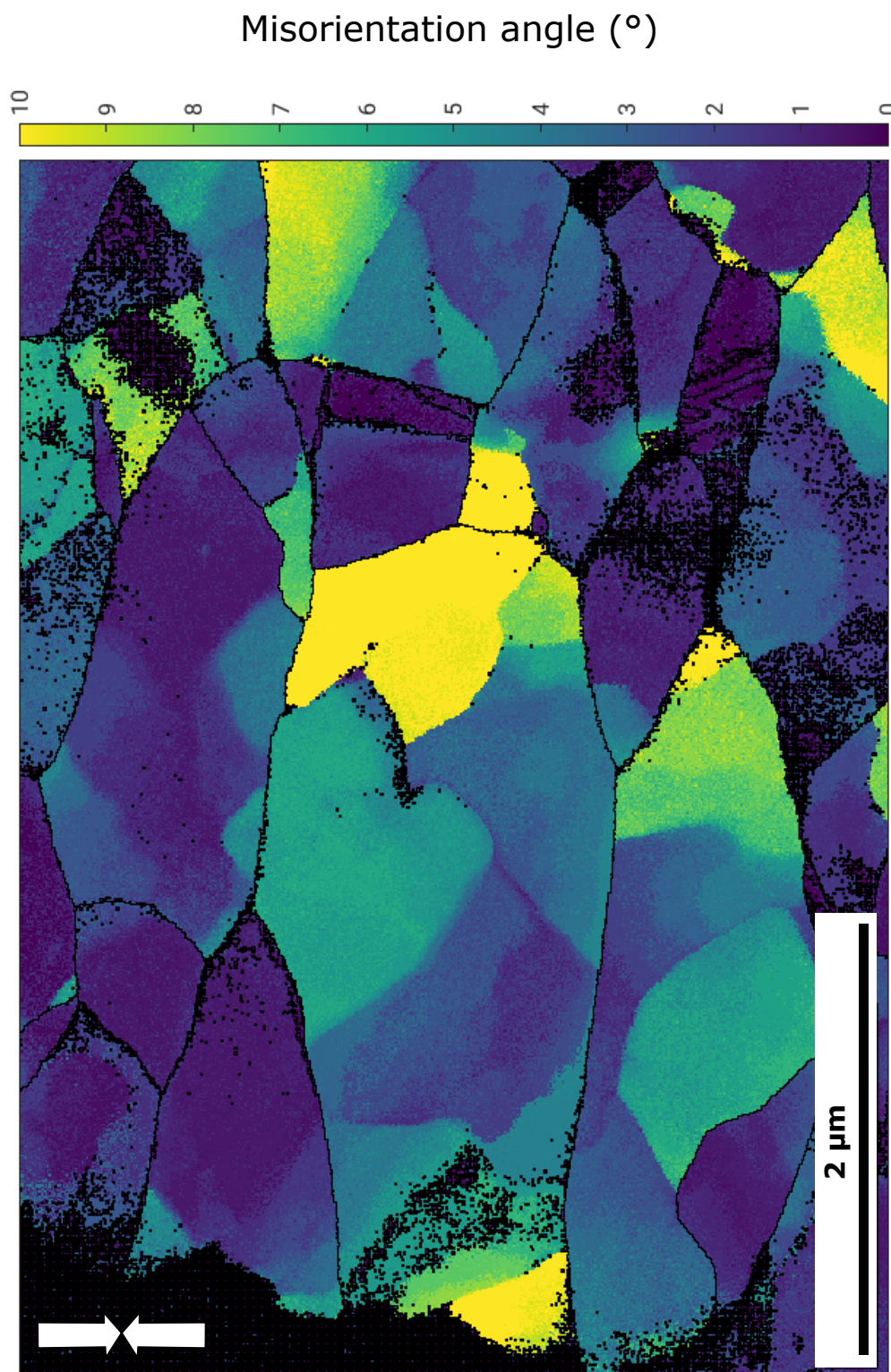


Figure S15. ASTAR intracrystalline misorientation map (GROD) for sample D2321, deformed at 1070 K and 2.5 GPa, in full size. The compression direction is indicated by the white arrows.

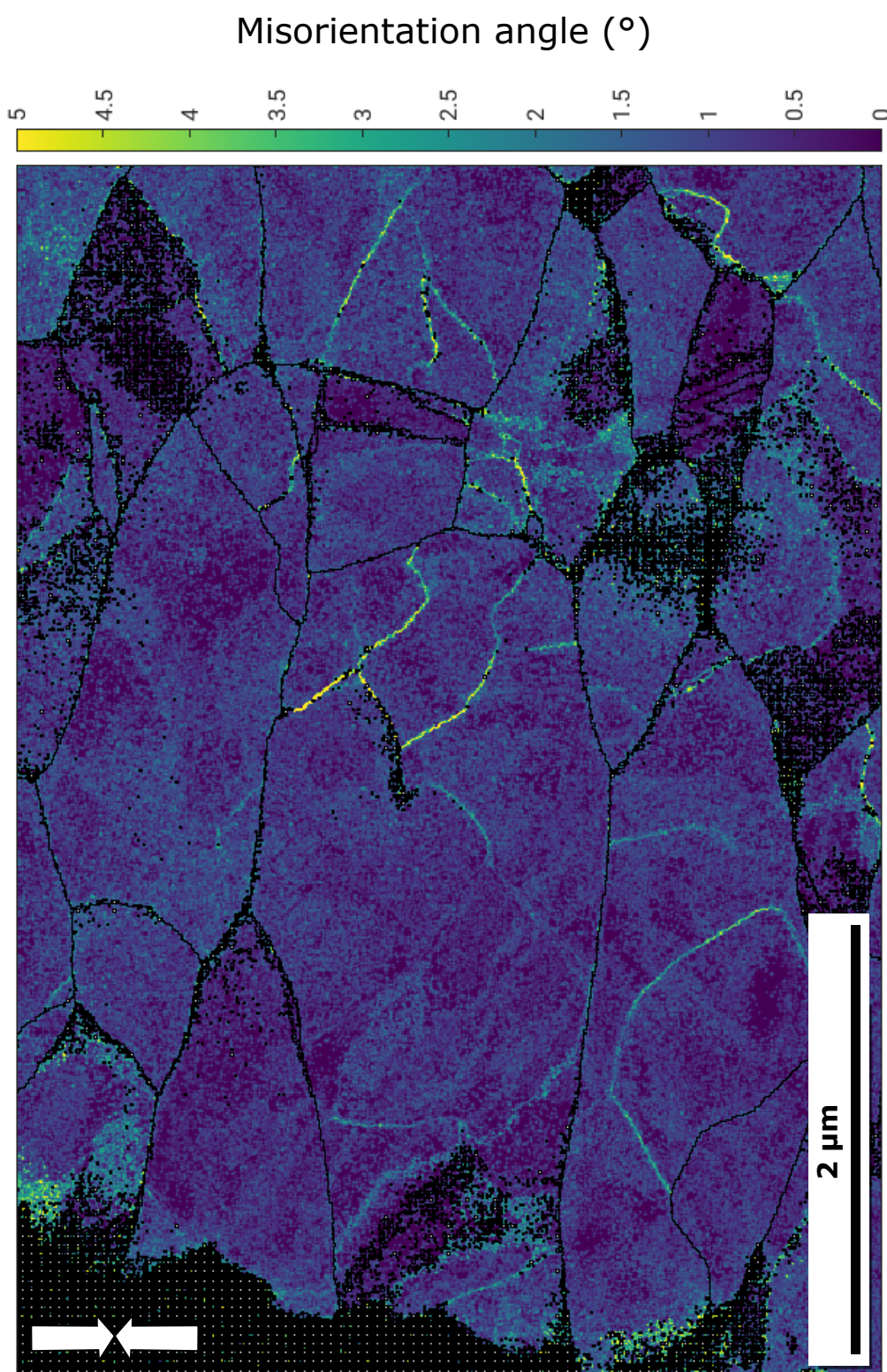


Figure S16. ASTAR local misorientation gradient (KAM) map for sample D2321, deformed at 1070 K and 2.5 GPa, in full size. The compression direction is indicated by the white arrows.